Corrosion Science 141 (2018) 14–17

Contents lists available at ScienceDirect

Corrosion Science

journal homepage: www.elsevier.com/locate/corsci

Short Communication

The effect of Sn–VO defect clustering on Zr alloy corrosion

B.D.C. Bell[a], S.T. Murphy[b], R.W. Grimes[a], M.R. Wenman[a,*]

[a] Department of Materials and Centre for Nuclear Engineering, Imperial College, London SW7 2AZ, UK
[b] Department of Engineering, Engineering Building, Lancaster University, Lancaster LA1 4YW, UK

ARTICLE INFO

Keywords:
Density functional theory
Zirconium
Niobium
Corrosion
Hydrogen pick-up

ABSTRACT

Density functional theory simulations were used to study Sn defect clusters in the oxide layer of Zr-alloys. Clustering was shown to play a key role in the accommodation of Sn in ZrO_2, with the $\{Sn_{Zr}{:}V_O\}^{\times}$ bound defect cluster dominant at all oxygen partial pressures below 10^{-20} atm, above which $Sn_{Zr}^{\times}$ is preferred. $\{Sn_{Zr}{:}V_O\}^{\times}$ is predicted to increase the tetragonal phase fraction in the oxide layer, due to the elevated oxygen vacancy concentration. As corrosion progresses, the transition to $Sn_{Zr}^{\times}$, and resultant destabilisation of the tetragonal phase, is proposed as a possible explanation for the early first transition observed in Sn-containing Zr–Nb alloys.

1. Introduction

Since the very beginning of water cooled-reactors zirconium has been the fuel cladding material of choice because it offers the best combination of neutronic, structural and corrosion properties. The first alloy regularly used in power reactors was Zircaloy-2, which contains 1.2 wt.% Sn [1,2]. Sn was originally included as a way to mitigate the detrimental effect on corrosion associated with the N and C impurities present in the Zr-sponge, however Sn was also found to improve strength and creep resistance, and was included in the later developed Zircaloy-4 and ZIRLO alloys [1–3].

Modern Zr-sponge contain significantly less impurities, and it has been established that a reduction in Sn concentration improves the corrosion resistance of Zr–Nb alloys. For this reason it has been removed from many alloys such as M5 [4]. The role of Sn in corrosion is still poorly understood, however work performed by Wei et al. [5] has shown that Sn does not influence the corrosion kinetics of Zr–Nb alloys, but rather that the removal of Sn delays the onset of transition. This behaviour does seem to be limited to Zr–Nb alloys as Ortner et al. [6] did not observe this behaviour in a study of Zircaloy-4 and it is noted that Zr–Nb–Sn alloys seem to behave quite differently to the Zircaloy series of alloys. Further, X-ray diffraction (XRD) measurements have shown that the tetragonal ZrO_2 phase fraction increases with increasing Sn content in Nb containing alloys [5]. Garner et al. suggested that Sn incorporated into the oxide may therefore be one of the stabilising features of this oxide phase; other contributions are from the compressive stress, generated on transformation of metal to oxide, and the possibly very small (nano-scale) size of some tetragonal grains [7]. Recent density functional theory (DFT) studies of the role of Sn in changing the defect concentrations showed that Sn can be present in either the 2+ or 4+ charge states and that there was a critical oxygen partial pressure at which point Sn^{2+}, present at low oxygen partial pressures, would switch to Sn^{4+} in the oxide layer [8]. Hulme et al. used X-ray absorption near edge spectroscopy (XANES) to prove that Sn^{2+} did indeed exist in the oxide layer but were not able to determine any depth profile for the 2+/4+ charge states for Sn [9]. It was postulated in both papers that Sn^{2+} may have created charged oxygen vacancies to charge balance the Sn^{2+} cations and the presence of these oxygen vacancies in turn stabilised the tetragonal phase. As the oxide layer thickens and the oxygen partial pressure increases (i.e. at a position in the oxide that is further from the metal-oxide interface) it was postulated that Sn^{2+} changes to Sn^{4+} on reaching a critical value and the vacancies were no longer needed for charge balance. This change in oxidation state of the Sn cations, and the associated drop in the oxygen vacancy concentration, destabilised the tetragonal phase and led to its transformation to the monoclinic phase and this in turn could have initiated cracking in the oxide associated with the transition because of the 4% volume increase from the tetragonal to monoclinic phases. The issue with this initial theory is it did not explain why the corrosion rate does not increase with increased oxygen vacancy concentration - something that was observed by Bell et al. when Zr is doped with Sc^{3+} ions [10].

In this paper a set of defects are modelled in tetragonal ZrO_2 using the same technique employed by Bell et al. [8,10,11]. These defects are bound $\{Sn_{Zr}{:}V_O\}$ clusters of different configurations and charge states. It is shown that certain combinations have a strong binding energy and are favoured over the isolated Sn ion defects previously presented. The effect of non-equilibrium charge in the oxide layer is also investigated

* Corresponding author.
E-mail address: m.wenman@imperial.ac.uk (M.R. Wenman).

https://doi.org/10.1016/j.corsci.2018.06.020
Received 28 April 2017; Received in revised form 11 June 2018; Accepted 16 June 2018
Available online 20 June 2018
0010-938X/

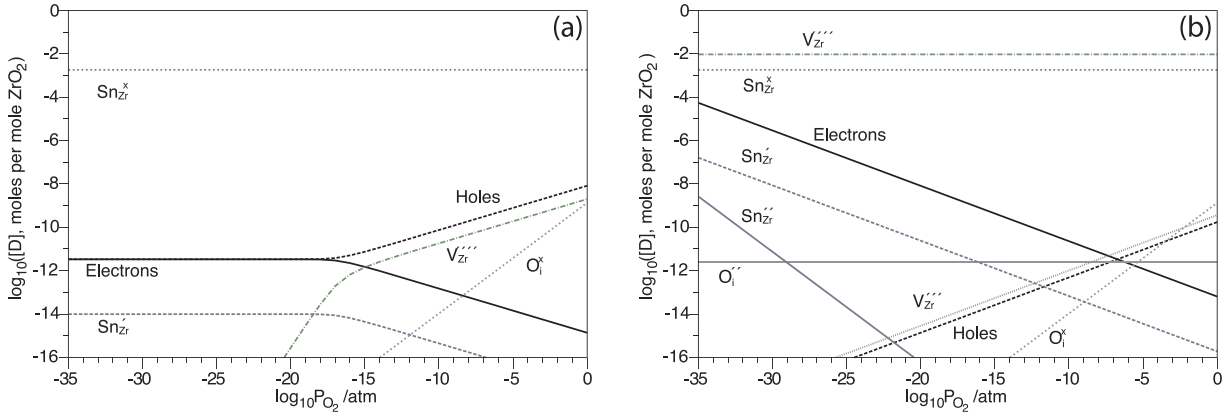

Fig. 1. Brouwer diagrams showing the predicted defect concentrations (plotted as the log of the concentration, in units of moles per mole of ZrO_2) in monoclinic ZrO_2 at 635 K doped with Sn at a concentration of 1×10^{-3} moles per mole of ZrO_2. The behaviour of the Sn dopant under equilibrium conditions is shown in (a). In (b) a space charge of 0.2 (moles of e^- per mole of ZrO_2) has been applied in order to investigate the behaviour under non-equilibrium charge conditions.

in the formulation of the Brouwer diagrams.

2. Methodology

DFT simulations were performed using the CASTEP 8.0 software [12], with ultra-soft pseudo potentials and a cut-off energy of 550 eV. The exchange-correlation functional was described by the Perdew, Burke and Ernzerhof (PBE) [13] formulation of the generalised gradient approximation (GGA). Integration of the Brillouin zone was performed using a Monkhorst–Pack sampling scheme [14], with a minimum *k*-point separation of 0.045 $Å^{-1}$. The Pulay method [15] for density mixing was employed.

Self-consistent calculations were performed until an energy convergence of 1×10^{-8} eV between successive iterations was achieved. The convergence criteria for geometry optimisation were; a maximum difference in energy of 1×10^{-5} eV, an atomic displacement of 5×10^{-4} Å between iterations and a maximum force between ions of 1×10^{-2} eV/Å.

Non-defective 108 atom t-ZrO_2 and 96 atom m-ZrO_2 supercells were geometry optimised under constant (zero) pressure, from which all defective structures were subsequently generated and the energy minimised under constant volume. An energy correction calculated using the screened Madelung method [16] was used to account for the electrostatic self-interaction of defects created by the use of periodic conditions and a finite supercell size using dielectric values calculated by Zhao and Vanderbilt [17].

Each single and clustered defect in each overall charge state of interest was simulated in isolation in a supercell of the requisite ZrO_2 phase. Defect clusters consisting of a substitutional Sn atom, Sn_{Zr}, and an oxygen vacancy, V_O, (i.e. $\{Sn_{Zr}{:}V_O\}$) were prepared by removing the nearest O ion to the Sn_{Zr} defect. The overall charge on the cluster was varied from −2 to +2 so that the Sn ion is able to assume a range of possible oxidation states. Defect formation energies (E^f) were calculated for each defect simulated using the methodology outlined in [8]. The calculated formation energies for each isolated defect were then used to approximate the interactions between multiple defects, as would be expected in a real oxide layer.

In any given defective cell, the sum of all defects multiplied by their charge must equal zero, since there is no overall charge on the crystal. This can be expressed as follows:

$$\sum_i q_i c_i - N_c \exp\left(-\frac{E_g - \mu_e}{k_B T}\right) + N_v \exp\left(-\frac{\mu_e}{k_B T}\right) = 0 \quad (1)$$

where the first term is the sum of the charges of all ionic defects (q_i is the ionic charge and c_i the concentration of ionic defect *i*), the second term is the electron concentration and the third term the hole concentration in the crystal. N_c and N_v are the density of states for the conduction and valence bands, E_g is the band gap of the crystal, μ_e is the electron chemical potential, k_B is the Boltzmann constant and T the temperature. The concentrations c_i of each ionic defect *i* are calculated using the approach developed by Kasamatsu et al. [18], which uses standard Boltzmann statistics to calculate concentrations but also accounts for ionic defects competing for the same lattice site.

Tetragonal ZrO_2 is a wide band gap insulator, and as such the concentrations of electrons and holes are expected to be sufficiently low that Boltzmann statistics are appropriate. Self-trapping of electrons causes a reduction in the formation energy of electrons in the conduction band, when compared to the value calculated by $E_g - \mu_e$, however due to the wide band gap the difference in energy is minimal and so this is an acceptable approximation [19].

Using the relationship in Equation (1), the electron chemical potential required to ensure charge neutrality for a given set of chemical potentials and oxygen partial pressure, and thus the concentration of all defects ([D]), can be calculated. The chemical potentials of the reactive species were obtained from formation energies of the relevant oxides following established methods [8,19–22]. The predicted defect concentrations as a function of oxygen partial pressure were then plotted for each oxide to produce Brouwer diagrams. As oxygen partial pressure in the oxide layer decreases with distance from the oxide/water interface, a Brouwer diagram can provide insight into the defect concentrations through the thickness of the oxide. For all diagrams, the DFT predicted band gaps of 3.40 eV for the monoclinic phase and 3.95 eV for the tetragonal phase were used.

The approach used in this work follows the methodology outlined in previous work by Bell et al. [8,10,11].

3. Results and discussion

Fig. 1 shows the predicted defect behaviour for monoclinic ZrO_2 doped with Sn at a concentration of 1×10^{-3} moles per mole ZrO_2. This Sn concentration, while lower than what would generally be expected for the oxide layer, was chosen to be sure that the solubility limit in the oxide phase was not exceeded. Across all oxygen partial pressures and despite the application of a high concentration of non-equilibrium charge to the system (see Fig. 1b), $Sn^{\times}_{Zr}$ is predicted to be the dominant defect type. This suggests that regardless of the local conditions, Sn in monoclinic ZrO_2 should only be observed in the 4+ oxidation state.

Previous work, investigating the behaviour of Sn in tetragonal ZrO_2, suggested that Sn can exist in both 2+ and 4+ oxidation states in the tetragonal phase and that the influence of oxygen vacancies could be significant [8]. Fig. 2 suggests that while $Sn^{\times}_{Zr}$ remains the dominant Sn defect at high oxygen partial pressures, below 10^{-20} atm the